



Preparation of polypyrrole–TiO₂ and its adsorption and photocatalytic degradation of salicylic acid

Huiqin Wang^a, Xiaolin Liu^{b,c}, Xinlin Liu^a, Pengwei Huo^{b,*}, Qingfeng Guan^{a,*}

^a*School of Materials Science & Engineering, Jiangsu University, Zhenjiang 212013, P.R. China, email: guangjszj@163.com (Q. Guan)*

^b*School of Chemistry & Chemical Engineering, Jiangsu University, Zhenjiang 212013, P.R. China, Tel. +86 511 8879 0187; Fax: +86 511 8879 1108; email: huopw1@163.com (P. Huo)*

^c*School of Biology and Chemical Engineering, Jiangsu University of Science and Technology, Zhenjiang 212003, China*

Received 1 October 2013; Accepted 21 March 2014

ABSTRACT

Polypyrrole–TiO₂ composited photocatalysts have been prepared by sol–gel method. The as-prepared photocatalysts were characterized by scanning electron microscopy, X-ray diffraction, and FT-IR. The results showed that the polypyrrole–TiO₂ consists of well-defined hollow tubes with the size of inner diameter 0.5–1 μm, and the hollow tubes exhibited non-crystal phase and it was well-formed anatase phase at high temperature treatment. The performances of polypyrrole–TiO₂ were tested by adsorption and degradation of salicylic acid. The adsorption equilibrium data, at different temperatures, were described by the Langmuir, Freundlich, Temkin and Dubinin–Radushkevich isotherm models. The results showed that the Langmuir model was well fit to the equilibrium adsorption data, and the adsorption capacities could reach 32.4 mg g⁻¹. The photocatalytic degradation activity of salicylic acid with polypyrrole–TiO₂ was investigated under visible light irradiation. It was revealed that the degradation rate of salicylic acid with the polypyrrole–TiO₂ which synthesized at 5°C without heat treatment could reach 48.6%. And the kinetics of photocatalytic degradation obeyed second-order kinetics.

Keywords: Polypyrrole–TiO₂; Adsorption; Photocatalysis; Degradation; Salicylic acid

1. Introduction

Salicylic acid is a key additive in many skin-care ointments, creams, gels, and transdermal patches, and it is applied in the scientific experiments widely. Therefore, the salicylic acid is easy to discharge into environment along with the large usage and increasing production, especially the water environment. Wastewater containing salicylic acid originates mainly from the synthesis of salicylic acid and its derivatives and

from rinsing of medical and cosmetic manufacture equipment [1]. And it may interact with living beings, which may generate toxic effects, destroy the endocrine system [2,3]. Therefore, it requires innovative technologies for disposing of salicylic acid. Photocatalytic oxidation is one of advanced oxidation processes based on the action of positively charged and holes on the surface of illuminated semiconductor, which possess high oxidation, and it could eliminate most pollutants, thus it was an effective way to resolve the salicylic acid pollution. And it has been widely attracted by many

*Corresponding author.

researchers owing to its potential application in purifying water and air. Among all of photocatalysts, Titanium dioxide (TiO_2), due to its strong oxidizing power, high photostability, commercially available, nontoxic, and redox selectivity, is one of the most popular and promising materials in photocatalysis [4–6]. However, the large intrinsic band gap energy (3.2 eV for anatase) and narrow photoresponse of TiO_2 limit the photocatalytic activity in ultraviolet light range. In response to the defect, much effort has been devoted to the modification of TiO_2 , such as doping ions, compound, dye sensitization, and organic substance [7–10]. The properties of delocalized conjugated structures in electron-transfer processes have been widely studied to show that they could effectively active a rapid photoinduced charge separation and a relatively low charge recombination [11]. As follow the conducting polymer, due to their diverse structures, special doping mechanism and optical properties, have been considered as new class of materials [12,13]. They have a large variety of applications in batteries, electrochemical display, and light-emitting diodes [13–15]. The conjugated polymers have extended *p*-conjugated electron systems such as polyaniline, polythiophene, polypyrrole (PPy), and their derivatives, due to their high absorption coefficients in the visible range of the spectrum, high mobility of charge carriers, and excellent stability, shown great promises [16,17]. Thus, it can be used to prepare modified TiO_2 materials which may improve the performance of TiO_2 .

To the best of our knowledge, most of the methods proposed to prepare PPy– TiO_2 need multi-steps, time-consuming, or expensive facilities. In the present work, PPy– TiO_2 was synthesized by sol–gel method. The photocatalytic process mainly contains two processes: first adsorption and second photodegradation, therefore, the adsorption and photocatalytic processes were investigated in photocatalytic degradation salicylic acid. The dynamic adsorption process was evaluated in the dark and the photocatalytic process was investigated under visible light irradiation after adsorption equilibrium. In order to study the adsorption process, the equilibrium adsorption data were analyzed using different adsorption isotherm models and kinetic equations. The photocatalytic activity of PPy– TiO_2 was evaluated by degradation of salicylic acid under visible light irradiation. And the kinetics of photocatalytic degradation was also discussed.

2. Experiment

2.1. Materials and characterization

Pyrrole (CAS number: 109-97-7. Chemically pure), 30% Perhydrol solution (CAS number: 7,722-84-1. Analytical Reagent (AR)), salicylic acid (CAS number:

69-72-7. AR), and ethanol (CAS number: 64-17-5. AR) were all purchased from Shanghai Chemical Reagent Co. and used as received. Titanium (IV) oxysulfate-sulfuric acid hydrate (CAS number: 123334-00-9) was purchased from Aladdin Chemistry Co. Ltd. Distilled water was used throughout this work.

The scanning electron microscopy (SEM) images were examined by S-4800 SEM (HITACHI, Japan). X-ray diffraction (XRD) technique was used to characterize the crystal structure. In this work, XRD patterns were obtained with a D8 ADVANCE X-ray diffractometer (Bruker AXS Company, Germany) equipped with Ni-filtrated Cu $K\alpha$ radiation (40 kV, 30 mA). The 2θ scanning angle range was 10° – 80° with a step of $0.04^\circ/0.4$ s. Infrared spectra ($4,000$ – 400 cm^{-1}) were recorded on a Nicolet NEXUS-470 FT-IR apparatus (USA).

2.2. Preparation of photocatalyst

The PPy– TiO_2 has been prepared by sol–gel method. About 1.73 g TiOSO_4 was added in 80 mL hydrochloric acid (pH 1) under mechanical agitation at different temperatures (5, 10, and 25°C) until transparent solution was obtained. And then 3.5 mL Pyrrole was injected into the mixture. After that, 3.9 mL perhydrol solution (30%) was dropwise added into the above mixture with constant agitation. At last, the resulting mixture was agitated for 6 h at different temperatures (5, 10, and 25°C). After reaction, the precipitates were washed with distilled water and alcohol for many times. Finally, the product was dried in an air at 60°C for 12 h. The samples were signed as PPy– TiO_2 (5°C), PPy– TiO_2 (10°C), and PPy– TiO_2 (25°C).

2.3. Photocatalysis experiments

The photodecolorization reactor of salicylic acid was carried out at 25°C in a photocatalytic reactor [18] under visible light. The photochemical reactor contained 0.1 g catalyst and 100 mL different concentration salicylic acid solution. After 20 min in the dark, it reached adsorption balance, its initial absorbency was determined. The photocatalytic reaction was initiating with one 500 W xenon lamp (wavelength range 400–780 nm), the illuminance of the Xenon lamp is $1,700$ – $1,800$ Lm m^{-2} . The samples were conducted in 20 min interval under visible light, which the reaction time was 100 min. And the residual amount of salicylic acid in the aqueous phase was determined using UV–vis spectrophotometer at $\lambda_{\text{max}} = 296$ nm. The photocatalytic degradation rate (DR) was calculated by this formula:

$$DR = (1 - A_i/A_0) \times 100\% \quad (1)$$

where A_0 is the initial absorbance of salicylic acid solution and A_i is the absorbance of reaction solution.

2.4. Batch mode adsorption studies

The factors of experimental parameters initial concentration and temperature on the adsorption removal of salicylic acid were studied. In study of adsorption kinetics, 5 mL of aqueous solution with initial salicylic acid with the 0.005 g of adsorbents in batch experiments, and the residual amount of salicylic acid in the aqueous phase was determined using UV-vis spectrophotometer at $\lambda_{\max} = 296$ nm. The amount of adsorption (mg g^{-1}) at time t was calculated by a mass balance relationship:

$$Q = \frac{(C_0 - C)V}{W} \quad (2)$$

where C_0 is the initial salicylic acid concentration (mg L^{-1}), C represents the residual concentration in solution at time t (mg L^{-1}), V is the solution volume (L), W is the adsorbent mass of TiO_2 (g), and Q is the absorptive amount (mg g^{-1}).

3. Results and discussion

3.1. Scanning electron microscopy

SEM is applied to obtain the detailed morphology of PPy-TiO₂ (5°C) (Fig. 1(a) and (b)), PPy-TiO₂ (10°C) (Fig. 1(c) and (d)), and PPy-TiO₂ (25°C) (Fig. 1(e) and (f)). As illustrated in Fig. 1((a) and (b)), PPy-TiO₂ (5°C) consist of well-defined hollow tubes that the size of inner diameter is 0.5–1 μm . Compared with PPy-TiO₂ (5°C), the inner diameter of PPy-TiO₂ (10°C) is smaller, which is influenced by the reaction temperature in the self assembly of sol-gel process. From Fig. 1((e) and (f)), it can be seen that PPy-TiO₂ (25°C) has been completely changed to different morphology and size distribution, furthermore PPy-TiO₂ (25°C) is conglomerate highly. Therefore, it can be found that reaction temperatures have much effect on the morphology of PPy-TiO₂. It maybe accelerates the reaction rate of sol-gel process with the higher temperatures and lead to poor self assembly, which is easy to conglomerate at high temperature, and show the disorder morphology.

3.2. X-ray diffraction

Fig. 2 shows XRD curves of PPy-TiO₂ (5°C) and PPy-TiO₂ (5°C) treated at different temperatures. The broad peak in the region of $2\theta = 20^\circ\text{--}30^\circ$ in XRD curve of PPy-TiO₂ (5°C) shows that the formed composite of polypyrrole and TiO₂ is amorphous. And different peaks appeared with increase in the treated temperature for the composite. The XRD patterns of PPy-TiO₂ (5°C) which was calcined at 500°C, shown seven peaks at 25.22°, 37.64°, 47.82°, 53.94°, 62.5°, 69.66°, and 75.02°, that can be indexed to the crystal planes of anatase TiO₂. Therefore, with increasing of calcination temperature, polypyrrole has been removed. And it is suggested that the composite without treated at high temperature contain polypyrrole and TiO₂.

3.3. FT-IR

FT-IR spectra of (a) PPy-TiO₂ (5°C), (b) PPy-TiO₂ (10°C), and (c) PPy-TiO₂ (25°C) are shown in Fig. 3. The broad peak at 3,110 cm^{-1} can be attributed to N-H stretching vibrations [9]. The peaks at 1,558 and 1,680 cm^{-1} are assignable to the C=C stretching vibrations of the PPy conjugation system [19], and the C-N stretching vibrations of PPy appeared at 1,210 cm^{-1} [20]. The peaks at 1,050, 926, and 796 cm^{-1} are symmetrical C-H in-plane bending, C-C inter-ring stretch, and N-H ring out of plane bending, respectively [21]. The results of FT-IR characterization show that PPy is successfully composited TiO₂ with sol-gel method.

3.4. The adsorption properties of PPy-TiO₂

The adsorption property of PPy-TiO₂ was evaluated by the removal of salicylic acid solution at 25°C. As shown in Fig. 4, PPy-TiO₂ (5°C) has more adsorption capacity of salicylic acid than the adsorption capacity of PPy-TiO₂ (10°C) and PPy-TiO₂ (25°C). The result shows that the morphology of PPy-TiO₂ is important to adsorption. PPy-TiO₂ (5°C), compared with PPy-TiO₂ (10°C) and PPy-TiO₂ (25°C), possesses higher adsorption performance, the reason may be due to the larger tube inner diameter, the more contact in the adsorption process. Fig. 5 illustrates the variation of 50 mg L^{-1} salicylic acid concentrations with time at different temperatures. As shown in Fig. 5, it can be seen that temperature is remarkably influenced the adsorption equilibrium of salicylic acid. And the adsorption of salicylic acid is decreased with increasing temperature, indicating that a low temperature is better for removal of salicylic acid with PPy-TiO₂ (5°C). The reduction of adsorption with rising temperature may be attributed to increase the molecules thermal motion and/or lead

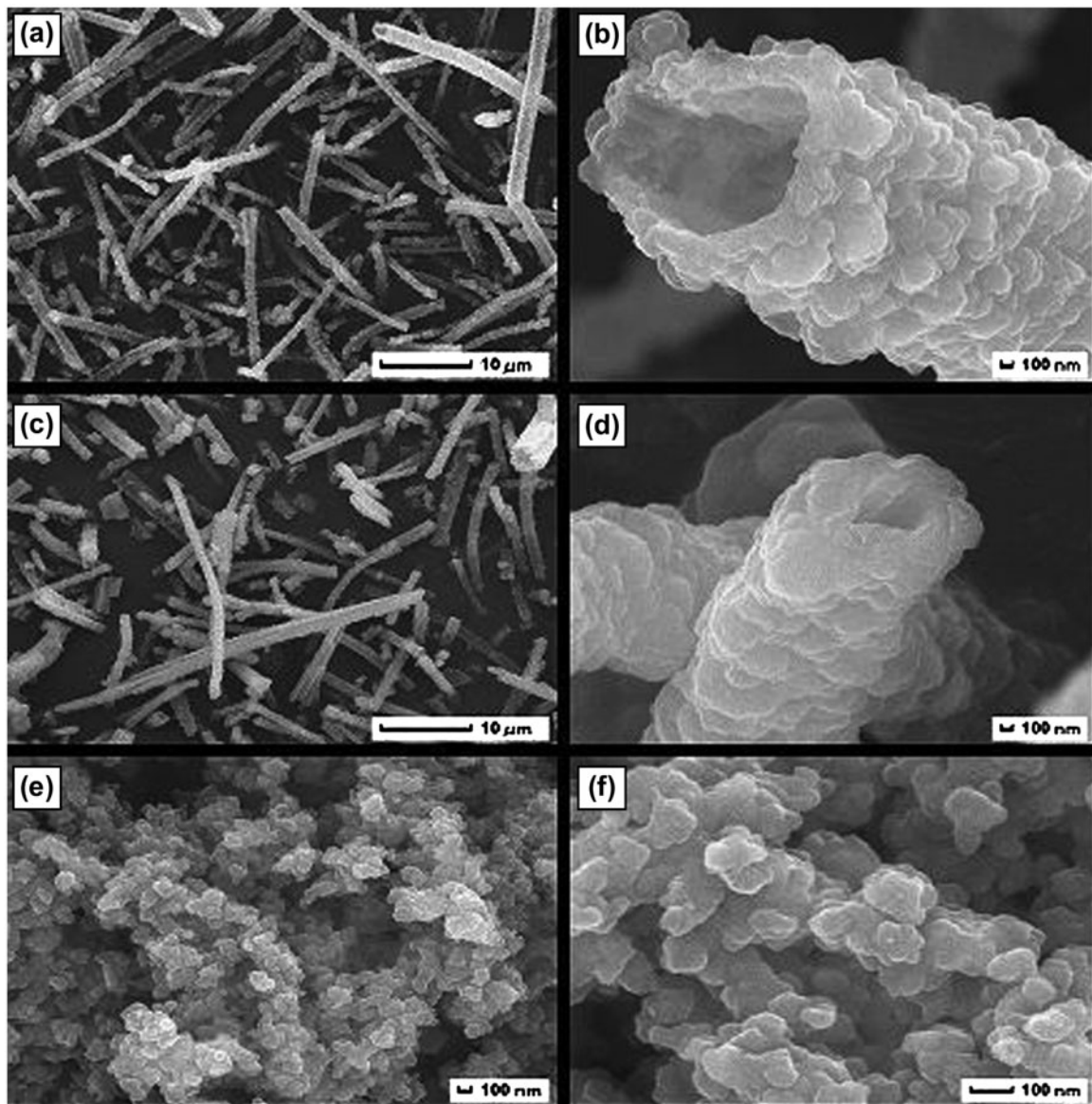


Fig. 1. The SEM images of different samples (a) and (b) PPy-TiO₂ (5°C), (c) and (d) PPy-TiO₂ (10°C), (e) and (f) PPy-TiO₂ (25°C).

to disadsorption, which is not easily adsorbed on the surface of PPy-TiO₂ (5°C). And the values of Q_e reduced with increasing temperature, which account for exothermic adsorption process. Therefore, the salicylic acid adsorption process is controlled by physical adsorption.

3.5. Adsorption isotherms

In the present study four isotherm equations, namely Langmuir [22], Freundlich [23], Temkin [24], and Dubinin-Radushkevich [25] isotherm were fitted to the experimental equilibrium data for PPy-TiO₂

(5°C) at different temperatures. It was studied by judging the correlation coefficient (R^2) for the adsorption behaviors. The results were shown in Table 1. Moreover, comparison of Langmuir, Freundlich, Temkin, and Dubinin-Radushkevich isotherm models for salicylic acid onto PPy-TiO₂ (5°C) using non-linear regression were also illustrated in Fig. 6. It can be seen that the adsorption capacity (Q_e) of PPy-TiO₂ (5°C) above all increased sharply, then increased slightly, and finally reached to maximum point. Furthermore, with temperature increased from 25 to 35°C and 45°C, Q_e of PPy-TiO₂ (5°C) was reduced obviously. It is possible that high temperature can increase the thermal motion

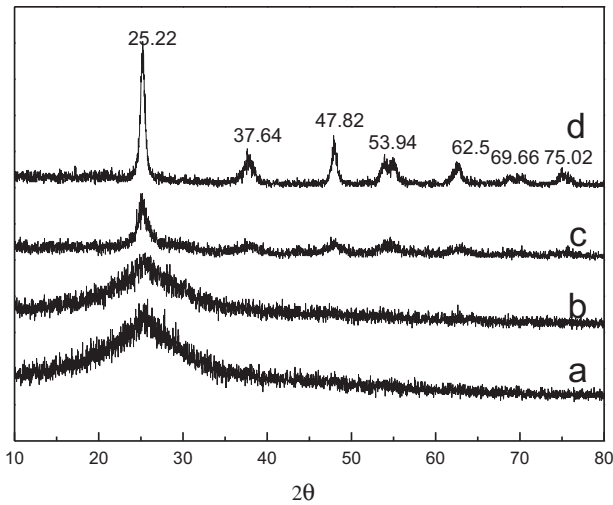


Fig. 2. XRD curves of (a) PPy-TiO₂ (5°C), (b) PPy-TiO₂ (5°C) was calcined at 300°C, (c) PPy-TiO₂ (5°C) was calcined at 400°C, and (d) PPy-TiO₂ (5°C) was calcined at 500°C.

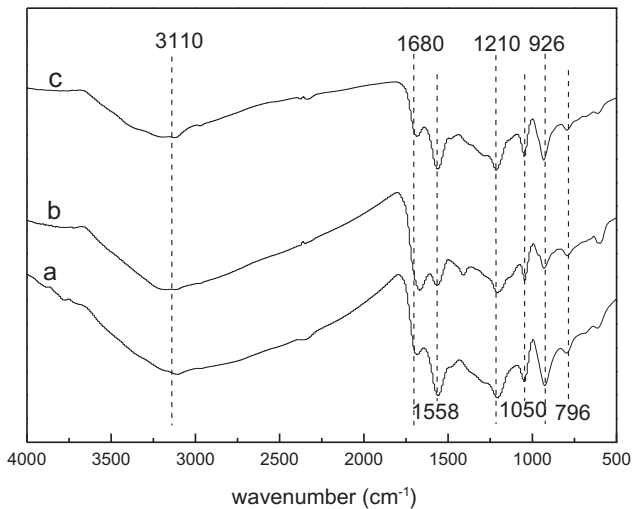


Fig. 3. FT-IR spectra of different samples (a) PPy-TiO₂ (5°C), (b) PPy-TiO₂ (10°C), and (c) PPy-TiO₂ (25°C).

of salicylic acid molecular and reduce the surface tension of solution. Moreover, PPy-TiO₂ (5°C) had better applicability for the Langmuir isotherm model, indicating monolayer molecular adsorption for salicylic acid with PPy-TiO₂ (5°C), and the adsorption capacities could reach 32.35 mg g⁻¹.

3.6. Adsorption kinetics

In order to investigate the mechanism of adsorption including mass transport and chemical reaction,

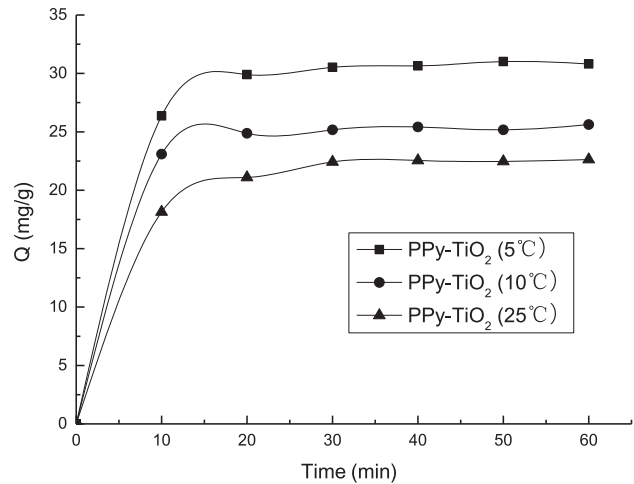


Fig. 4. The adsorption experiments of different samples at 50 mg L⁻¹ salicylic acid.

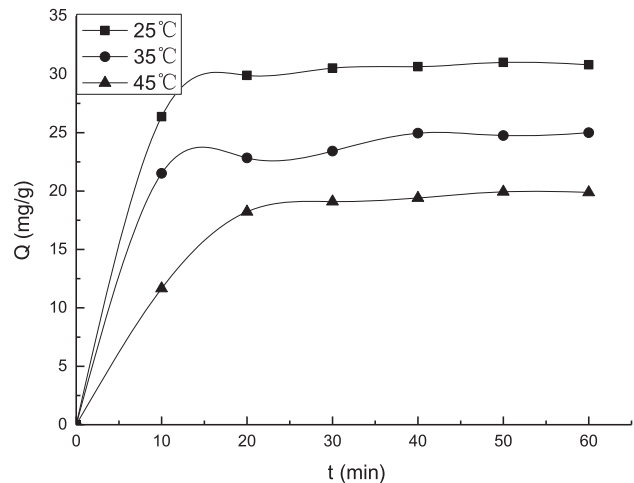


Fig. 5. The kinetics of adsorption at different temperature of salicylic acid by PPy-TiO₂ (5°C).

the pseudo-first-order equation and pseudo-second-order equation [26,27], were analyzed from the kinetic data. They are described in Eqs. (3) and (4):

$$\ln(Q_e - Q_t) = \ln Q_e - k_1 t \quad (3)$$

$$\frac{t}{Q_t} = \frac{1}{k_2 Q_e^2} + \frac{t}{Q_e} \quad (4)$$

Q_e and Q_t are the amount of salicylic acid onto sorbent at the equilibrium and time t (min), respectively. Values of k_1 and k_2 are calculated from the plot of $\ln(Q_e - Q_t)$ vs. t and t/q_t vs. t , respectively.

Table 1
Adsorption isotherm constants for salicylic acid with PPy–TiO₂

Adsorption isotherm models	Constants	298 K	308 K	318 K
Langmuir equation	$Q_{m,c}$ (mg g ⁻¹)	32.35	25.72	23.44
	R^2	0.9988	0.9987	0.9914
	K_L (L mg ⁻¹)	0.4755	0.4718	0.1230
	R_L	0.06349	0.07816	0.2897
Freundlich equation	R^2	0.9955	0.9987	0.9583
	K_F (mg g ⁻¹)	22.70	17.53	7.962
	n	12.42	17.53	4.204
Temkin	R^2	0.9958	0.9987	0.9674
	K_T (L mg ⁻¹)	7,943	3,135	2.097
	B_T	2.414	2.074	4.358
Dubinin–Radushkevich equation	$Q_{m,c}$ (mg g ⁻¹)	32.30	25.65	22.84
	R^2	0.9989	0.9976	0.9868
	K_{DR} (mol ² kJ ²)	1.630×10^{-4}	1.617×10^{-4}	5.110×10^{-4}
	E (kJ mol ⁻¹)	55.38	55.61	31.28

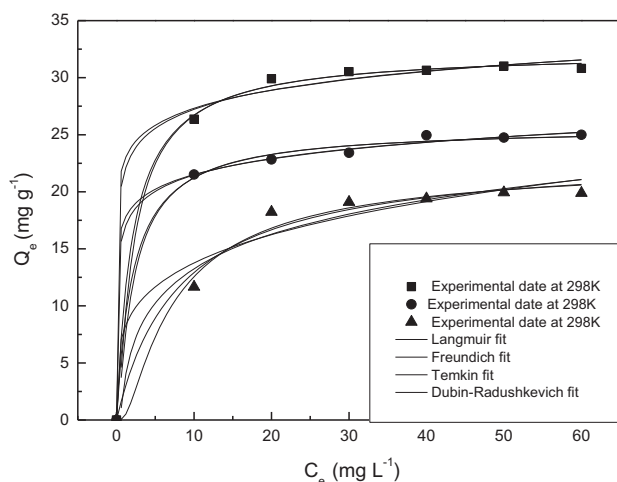


Fig. 6. Comparison of Langmuir, Freundlich, Temkin, and Dubinin–Radushkevich isotherm models for PPy–TiO₂ (5°C) using non-linear regression.

All the rate constants of adsorption and linear regression values were shown in Table 2. It can be found that the adsorption of salicylic acid onto PPy–TiO₂ (5°C) followed pseudo-first-order kinetics because of the well fit between experimental and calculated values of Q_e (all R^2 values above 0.99 at different temperatures). The adsorption kinetics of salicylic acid onto PPy–TiO₂ (5°C) has been well correlated by a pseudo-first-order and two step reaction mechanisms. The first reaction stage appears to be diffusion controlled and the second stage is chemical sorption controlled.

Fig. 7 illustrates the plot of the experimental data of the amount of salicylic acid adsorbed per unit mass of sorbent against time along the values for the

pseudo-first-order and pseudo-second-order kinetic model. As shown in Fig. 7, the equilibrium time required for the adsorption of salicylic acid from 50 mg L⁻¹ solution was about 30 min for PPy–TiO₂ (5°C) at different temperatures. And increasing temperature, initial adsorption rates decreased.

3.7. Photocatalytic activity and kinetic analysis

The photocatalytic activity of PPy–TiO₂ was evaluated by degradation of salicylic acid solution. As shown in Fig. 8, PPy–TiO₂ (5°C) shows better photocatalytic activity than PPy–TiO₂ (10°C) and PPy–TiO₂ (25°C) under visible light irradiation. Degradation percent after 120 min irradiation are 48.6, 42.4, and 35.7%. It shows that the morphology of photocatalysts is important to the photocatalytic activity. In order to study the kinetics of photodegradation process of salicylic acid, the first- and second-order kinetics were used to fit the experimental data, the results showed in Figs. 9 and 10, it can be found that the second-order kinetics the entire linear regression coefficient (R^2) is greater than the first-order kinetics, photocatalytic degradation of salicylic acid obeyed second-order kinetics. The rate constant value of 10 mg L⁻¹ salicylic acid was 1.11×10^{-2} (mol m⁻³)⁻¹ S⁻¹. The experimental data can be rationalized in terms of the modified form of Langmuir–Hinshelwood kinetic treatment, which has already been successfully used to describe solid–liquid reactions [28]. The rate of unimolecular surface reaction is proportional to the surface coverage assuming that the reactant is strongly adsorbed on the catalyst surface than the products [29]. It is shown that degradation process largely depends on the interfacial interaction of the photocatalyst surface [30].

Table 2
Kinetic constants for the pseudo-first-order equation and pseudo-second-order equation

Kinetic models		298 K	308 K	318 K
Pseudo-first-order equation	$Q_{e,c}$ (mg g^{-1})	30.74	24.35	20.13
	R^2	0.9998	0.9926	0.9935
	K_1 (L min^{-1})	0.1935	0.2043	0.09601
Pseudo-second-order equation	$Q_{e,c}$ (mg g^{-1})	32.35	25.73	23.44
	R^2	0.9988	0.9918	0.9815
	K_2 ($\text{g g}^{-1} \text{min}^{-1}$)	0.0147	0.0183	0.00525

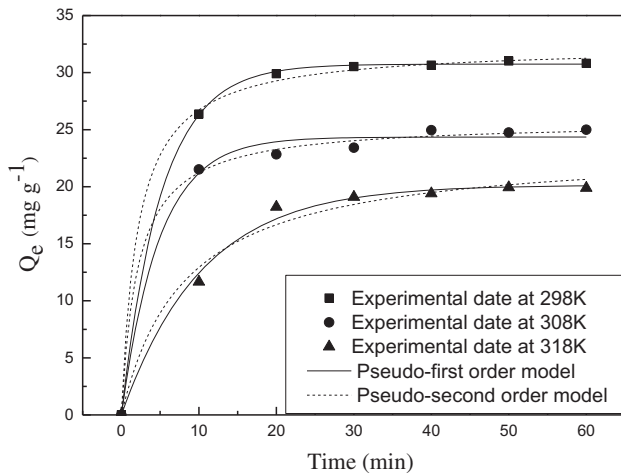


Fig. 7. Kinetic models for the effect of temperature on adsorption of PPy-TiO₂ (5°C).

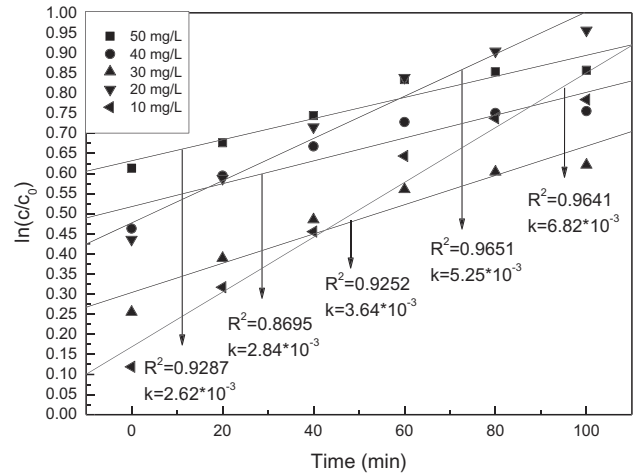


Fig. 9. The first kinetic of PPy-TiO₂ at different initial concentration salicylic acid.

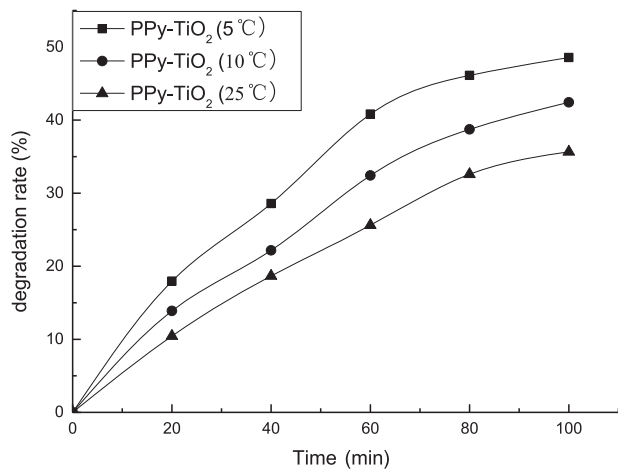


Fig. 8. The photocatalytic experiments of different samples at 10 mg L^{-1} salicylic acid.

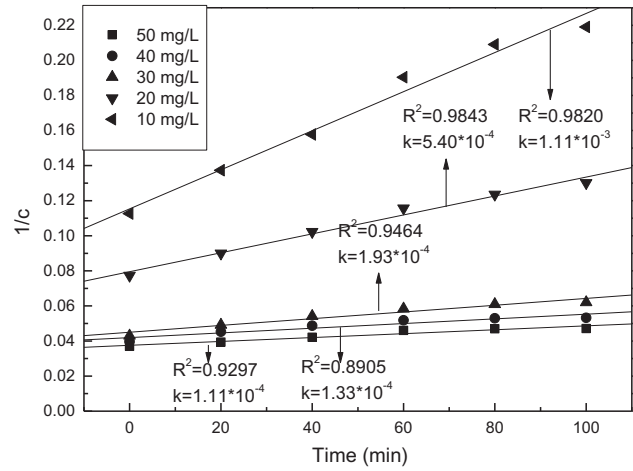


Fig. 10. The second kinetic of PPy-TiO₂ at different initial concentration salicylic acid.

4. Conclusion

In this work, PPy–TiO₂ was synthesized by sol–gel method. From the characterization, the results indicated that PPy–TiO₂ (5 °C) consists of well-defined hollow tubes. The performance of polypyrrole–TiO₂ was determined by adsorption of salicylic acid in dark, and degradation of salicylic acid under visible light irradiation. The adsorption thermodynamics and kinetics were investigated. The isotherms exhibited the Freundlich behavior at all temperatures, indicating monolayer molecular adsorption for salicylic acid with PPy–TiO₂ (5 °C). And the kinetics of adsorption followed the pseudo-first-order model. After adsorption equilibrium, the photocatalytic DR of salicylic acid with PPy–TiO₂ (5 °C) could reach 48.6%. And the kinetics of photocatalytic degradation obeyed second-order kinetics. The rate constant value of 10 mg L⁻¹ salicylic acid was $1.11 \times 10^{-2} \text{ (mol m}^{-3}\text{)}^{-1} \text{ s}^{-1}$.

Acknowledgments

We gratefully acknowledge the financial support of the National Natural Science Foundation of China (No. 21207053), the Natural Science Foundation of Jiangsu Province (BK2011460, BK20130489), the Specialized Research Fund for the Doctoral Program of Higher Education (20113, 227110019), China Postdoctoral Science Foundation (2012M511219, 2011M500869).

References

- [1] A. Goi, Y. Veressinina, M. Trapido, Degradation of salicylic acid by Fenton and modified Fenton treatment, *Chem. Eng. J.* 143 (2008) 1–9.
- [2] W.-L. Chou, C.-T. Wang, K.-Y. Huang, T.-C. Liu, Electrochemical removal of salicylic acid from aqueous solutions using aluminum electrodes, *Desalination* 271 (2011) 55–61.
- [3] A.I. Balcioglu, M. Ötker, Treatment of pharmaceutical wastewater containing antibiotics by O₃ and O₃/H₂O₂ processes, *Chemosphere* 50 (2003) 85–95.
- [4] A.F. Marye, T.D. Maria, Heterogeneous photocatalysis, *Chem. Rev.* 93 (1995) 341–357.
- [5] M.R. Hoffmann, S.T. Martin, W. Choi, D.W. Bahnemann, Environmental applications of semiconductor photocatalysis, *Chem. Rev.* 95 (1995) 69–96.
- [6] B. Ohtani, Y. Ogawa, S.-I. Nishimoto, Photocatalytic activity of amorphous–anatase mixture of titanium (IV) oxide particles suspended in aqueous solutions, *J. Phys. Chem. B* 101 (1997) 3746–3752.
- [7] Y. Ishibai, J. Sato, T. Nishikawa, S. Miyagishi, Synthesis of visible-light active TiO₂ photocatalyst with Pt-modification: Role of TiO₂ substrate for high photocatalytic activity, *Appl. Catal. B* 79 (2008) 117–121.
- [8] T. Matsunaga, H. Yamaoka, S. Ohtani, Y. Harada, T. Fujii, T. Ishikawa, High photocatalytic activity of palladium-deposited mesoporous TiO₂/SiO₂ fibers, *Appl. Catal. A-Gen.* 351 (2008) 231–238.
- [9] C. Zhang, Q.L. Li, J.Q. Li, Synthesis and characterization of polypyrrole/TiO₂ composite by *in situ* polymerization method, *Synth. Met.* 160 (2010) 1699–1703.
- [10] Z.Y. Wang, W.P. Mao, H.F. Chen, F.A. Zhang, X.P. Fan, G.D. Qian, Copper(II) phthalocyanine tetrasulfonate sensitized nanocrystalline titania photocatalyst: Synthesis *in situ* and photocatalysis under visible light, *Catal. Commun.* 7 (2006) 518–522.
- [11] G. Yu, J. Gao, J.C. Hummelen, F. Wudl, A.J. Heeger, Polymer photovoltaic cells: Enhanced efficiencies via a network of internal donor–acceptor heterojunctions, *Science* 270 (1995) 1789–1791.
- [12] R. Gangopadhyay, A. De, Conducting polymer nanocomposites: A brief overview, *Chem. Mater.* 12 (2000) 608–622.
- [13] H. Nguyen Conga, V. de la Garza Guadarrama, J.L. Gautier, P. Chartier, Ni_xCo_{3-x}O₄ Mixed valence oxide nanoparticles/polypyrrole composite electrodes for oxygen reduction, *J. New Mat. Electrochem. Syst.* 5 (2002) 35–40.
- [14] Y. Cao, P. Smith, A.J. Heeger, Counter-ion induced processibility of conducting polyaniline and of conducting polyblends of polyaniline in bulk polymers, *Synth. Met.* 48 (1992) 91–97.
- [15] H. Nguyen-Cong, V. de la Garza Guadarrama, J.J. Gautier, P. Chartier, Oxygen reduction on Ni_xCo_{3-x}O₄ spinel particles/polypyrrole composite electrodes: Hydrogen peroxide formation, *Electrochim. Acta* 48 (2003) 2389–2395.
- [16] H.C. Liang, X.Z. Li, Visible-induced photocatalytic reactivity of polymer-sensitized titania nanotube films, *Appl. Catal. B* 86 (2009) 8–17.
- [17] A. Pron, P. Rannou, Processible conjugated polymers: From organic semiconductors to organic metals and superconductors, *Prog. Polym. Sci.* 27 (2002) 135–190.
- [18] P. Huo, X. Gao, Z. Lu, X. Liu, Y. Luo, W. Xing, J. Li, Y. Yan, Photocatalytic degradation of antibiotics in water using metal ion@TiO₂/HNTs under visible light, *Desalin. Water Treat.* (2013), doi: [10.1080/19443994.2013.822327](https://doi.org/10.1080/19443994.2013.822327).
- [19] D.Y. Kim, J.Y. Lee, D.K. Moon, C.Y. Kim, Synthesis and characterization of polypyrrole/TiO₂ composite by *in situ* polymerization method, *Synth. Met.* 160 (2010) 1699–1703.
- [20] H. Shiigi, M. Kishimoto, H. Yakabe, B. Deore, T. Nagaoka, Highly selective molecularly imprinted overoxidized polypyrrole colloids: One-step preparation technique, *Anal. Sci.* 18 (2002) 41–44.
- [21] R. Kostić, D. Raković, S.A. Stepanyan, I.E. Davidova, L.A. Gribov, Vibrational spectroscopy of polypyrrole, theoretical study, *J. Chem. Phys.* 102 (1995) 3104–3109.
- [22] M. Mazzotti, Equilibrium theory based design of simulated moving bed processes for a generalized Langmuir isotherm, *J. Chromatogr. A* 1126 (2006) 311–322.

- [23] S.J. Allen, G. McKay, J.F. Porter, Adsorption isotherm models for basic dye adsorption by peat in single and binary component systems, *J. Colloid Interface Sci.* 280 (2004) 322–333.
- [24] J.F. Gao, Q. Zhang, K. Su, R. Chen, Y.Z. Peng, Biosorption of acid yellow 17 from aqueous solution by non-living aerobic granular sludge, *J. Hazard. Mater.* 174 (2010) 215–225.
- [25] A.P. Terzyk, R. Wojsz, G. Rychlicki, P.A. Gauden, Fractal dimension of microporous carbon on the basis of Polanyi–Dubinin theory of adsorption. Dubinin–Radushkevich adsorption isotherm equation, *Colloids Surf. A* 119 (1996) 175–181.
- [26] Y.S. Ho, G. McKay, The sorption of lead(II) ions on peat, *Water Res.* 33 (1999) 578–584.
- [27] Y.S. Ho, G. McKay, Pseudo-second-order model for sorption processes, *Process Biochem.* 34 (1999) 451–465.
- [28] L.C. Chen, T.C. Chou, Kinetics of photodecolorization of methyl orange using titanium dioxide as catalyst, *Chem. Res.* 32 (1993) 1520–1527.
- [29] H. Al-Ekabi, N. Serpone, Kinetics studies in heterogeneous photocatalysis. I. Photocatalytic degradation of chlorinated phenols in aerated aqueous solutions over titania supported on a glass matrix, *J. Phys. Chem.* 92 (1988) 5726–5731.
- [30] W.L. Guo, X.L. Liu, P.W. Huo, X. Gao, D. Wu, Z.Y. Lu, Y.S. Yan, Hydrothermal synthesis spherical TiO_2 and its photo-degradation property on salicylic acid, *Appl. Surf. Sci.* 258 (2012) 6891–6896.